Quantifying individual (anti)bonding molecular orbitals' contributions to chemical bonding

*Jurgens H. de Lange, Daniël M.E. van Niekerk, Ignacy Cukrowski**

Department of Chemistry, Faculty of Natural and Agricultural Sciences, University of Pretoria, Lynnwood Road, Hatfield, Pretoria 0002, South Africa

Correspondence to: Ignacy Cukrowski (E-mail: ignacy.cukrowski@up.ac.za)

Electronic Supplementary Information

Table of content **Page**

Part 1

Theoretical background and development of the MO-ED and MO-DI methods

The MO-ED Method

The MO-ED method seeks to describe the total electron density, as well as its topology, in terms of molecular orbital density contributions. Specifically, we aim here to describe the presence of a density bridge, with its associated critical point, in terms of MO densities. To do so we will first review some preceding topics related to the topology of the electron density.

The topology of the electron density

Within the field of Quantum Chemical Topology (QCT), a critical point (CP) in the electron density (ED) at a coordinate $\mathbf{r}_c$ is a local maximum, minimum or a saddle point where the first derivative (and each of its three components) vanishes:

$$\nabla\rho(\mathbf{r}_c) = \mathbf{i}\frac{\partial\rho}{\partial x} + \mathbf{j}\frac{\partial\rho}{\partial y} + \mathbf{k}\frac{\partial\rho}{\partial z} = 0 \qquad (1)$$

Each CP is a local maximum or minimum along each of the three principle axes corresponding to maximum curvature. The type of CP can be determined by evaluating components of the Hessian matrix, which describe the partial second derivatives of the ED at $\mathbf{r}_c$:

$$\mathbf{A}(\mathbf{r}_c) = \begin{pmatrix} \frac{\partial^2\rho}{\partial x^2} & \frac{\partial^2\rho}{\partial x\partial y} & \frac{\partial^2\rho}{\partial x\partial z} \\ \frac{\partial^2\rho}{\partial y\partial x} & \frac{\partial^2\rho}{\partial y^2} & \frac{\partial^2\rho}{\partial y\partial z} \\ \frac{\partial^2\rho}{\partial z\partial x} & \frac{\partial^2\rho}{\partial z\partial y} & \frac{\partial^2\rho}{\partial z^2} \end{pmatrix} \qquad (2)$$

The Hessian matrix can be diagonalized to give three curvatures along the principle axes at $\mathbf{r}_c$, yielding three eigenvalues, λ_1, λ_2 and λ_3, and associated eigenvectors. The sign of each eigenvalue reveals whether $\mathbf{r}_c$ is a local minimum or maximum along the associated eigenvector, where positive and negative eigenvalues relate to local minima and maxima, respectively.

Each CP can be classified according to its partial first and second derivatives, and is given a rank, ω, and signature, σ. The rank determines the number of non-zero curvatures (eigenvalues of the Hessian matrix). In other words, a rank of (+3) indicates that a CP is a local maximum or

minimum in all three principle axes. The signature is the algebraic sum of the signs of the eigenvalues, and a signature of (–1) indicates that $\mathbf{r}_c$ is a local minimum in one axis but a local maximum in the remaining two axes (+1 –1 –1 = –1). While many CPs of rank 1 and 2 exist in any ED distribution, only a number of CPs of rank 3 will exist, subject to the Poincaré-Hopf relationship,[1] and rank 3 CPs are therefore of particular use in QCT.

The topology of the ED is generally dominated by the electrostatic attractive force between nuclei and electrons, and as such, every nuclear coordinate is marked by a (+3,–3) CP – a local maximum in all three principle axes. (+3,–1) CPs are often found between pairs of nuclei and are known as bond critical points (BCPs). CPs found within a ring of nuclei are (+3,+1) CPs, known as ring critical points (RCPs), and a CP enclosed by a number of ring critical points is always a (+3,+3) CP, known as a cage critical point (CCP).

QCT has revealed a peculiar property regarding the ED distribution between nuclei. A BCP is always observed at the interface between two zero-flux surfaces outside of the limit at infinity, *i.e.* interatomic zero-flux surfaces. Two gradient vectors originate at each of the enclosed nuclei and terminate at the BCP. The path defined by these two vectors is known as a density bridge (DB, also known as a *bond path* or a line path[2]). The ED is at a local maximum perpendicular to the DB at each and every coordinate of the DB. A DB is a remarkable yet still misunderstood property of the ED. The collection of DBs gives rise to a *molecular graph*, which defines QTAIM-based atomic connectivity.

Two of the eigenvalues of the Hessian matrix (λ_1 and λ_2) will be negative at each and every coordinate of a DB, indicating a negative partial second derivative along the principle vectors perpendicular to the DB itself. A negative partial second derivative at $\mathbf{r}$, $\frac{\partial^2 \rho(\mathbf{r})}{\partial \mathbf{r}^2}$, can be seen as a measure of local *concentration* of the ED, in that the ED at $\mathbf{r}$ is greater than the average of its neighbouring coordinates along a specific vector.[7] Along the DB, the third eigenvalue of the Hessian matrix (λ_3) will always be positive, indicating a local *depletion* of ED. Generally, at a given coordinate $\mathbf{r}$ along an internuclear vector and as long the two nuclei are not part of a cage, $\lambda_1 < 0$ and $\lambda_3 > 0$. The sign of the remaining eigenvalue, λ_2, then generally determines whether ED is concentrated at $\mathbf{r}$ relative to its neighbouring environment, thereby forming an DB if a CP is present, or whether the ED is depleted. Such concentrations and depletions have been used extensively by both QTAIM and other QCT techniques, such as the Noncovalent Interactions (NCI) technique,[3,4] to indicate '*attractive*' or *'repulsive*' interactions. However, some of us

previously showed[5] that measures of ED concentration utilising λ_2 is only a relative to the local environment where it is measured.

Cross-sections along λ_2–eigenvector

As stated above, the presence of a DB can be fully determined in most circumstances from investigation of i) the partial directional first derivative and ii) the sign of the partial directional second derivative of the ED along the eigenvector associated with the λ_2 eigenvalue of the Hessian matrix. We will henceforth refer to this eigenvector simply as the λ_2–eigenvector. We have previously noted[5,6] that the ED distribution, as well as decompositions of the ED, of cross-sections along this vector can provide tremendous information regarding *why* a DB for a particular chemical interaction is present or not. Specifically, the overall concentration or depletion of ED along the λ_2–eigenvector provides valuable information regarding the character of the interaction, and the individual concentration or depletion of ED decomposition products can provide insight into the underlying mechanics. Cross-sections along one of the other principle axes, *i.e.* λ_1– or λ_3–eigenvectors, can provide useful information regarding the ED concentration/depletion relative to different interatomic interactions.

Decomposition of ED and its topology in terms of MO densities

The ED can easily be decomposed in terms of canonical or natural molecular orbitals (MOs),

$$\rho(\mathbf{r}) = \sum_{i}^{N_{MO}} \nu_i |\chi_i(\mathbf{r})|^2 \qquad (3)$$

where χ_i is an MO with occupation ν_i. The coordinate **r** can be varied (specifically, in this case, along the λ_2–eigenvector) in order to measure the orbital contributions to the ED in a region of real-space, as well as then calculate partial directional first and second derivatives.

It is useful to define a consistent and universal coordinate, **r***, which can be used to quantify an orbital's ED contribution to any internuclear region in a transferable fashion. While there are potentially multiple different approaches to define such an **r***, we have decided to use the topology of the ED as a general guide. If a (3,–1) CP is present, then we define **r*** = $\mathbf{r_c}$, the coordinate of the CP. If a (3,–1) CP is not present, then we set **r*** to be the position of the minimum density point (MDP)[15], which is defined as the coordinate on an internuclear vector where the ED is at a minimum. The MDP is well-defined for any given atom-pair, and the MDP and BCP often coincides to the same coordinate unless the corresponding DB is particularly bent.

Next, we consider the partial directional second derivatives along the λ_2–eigenvector of each MO density as measured at **r***, $\frac{\partial^2 \nu_i |\chi_i(\mathbf{r}^*)|^2}{\partial \lambda^2}$. We can label each MO as concentrating ED (negative second derivative), depleting ED (positive second derivative), non-contributing to the ED (in the case of an MO node) or removing ED (in the case of negative occupations in multi-reference wavefunctions). The ED at **r*** can then be defined in terms of MO components with different characters:

$$\rho(\mathbf{r}^*) = \rho_{\text{concentrating}}(\mathbf{r}^*) + \rho_{\text{depleting}}(\mathbf{r}^*) + \rho_{\text{non-contributing}}(\mathbf{r}^*) + \rho_{\text{removing}}(\mathbf{r}^*) \quad (4)$$

Each individual MO's character is therefore defined relative to a specific internuclear region, as opposed to a "net" character given based on inspection of molecular-wide isosurface or interference patterns of atomic orbitals. In the main body of this text, we investigate the similarities of orbitals with similar characters for various di- and polyatomic moleucles.

The MO-DI Method

The MO-DI method describes the QTAIM-defined delocalization index in terms of MO contributions to the pair-density. We will first review the basic concepts of how delocalization indices are calculated within QTAIM.

The integration of the overlap between all MO pairs over a QTAIM-defined atomic domain, Ω(A), can be written as a matrix associated with atom A, $\mathbf{S}^{\mathrm{A}}$, and is known as an *atomic overlap matrix* (AOM).[1] The elements of an N_{MO} by N_{MO} atomic overlap matrix,

$$S_{ij}^{\mathrm{A}} = \sum_{ij} \int_{\mathrm{A}} \sqrt{\nu_i}\sqrt{\nu_j}\chi_i^*(\mathbf{r})\chi_j(\mathbf{r})d\mathbf{r} \quad (7)$$

provide information on how each MO (diagonal elements) or a MO-pair (off-diagonal elements) contribute to the ED distribution of atom A. The atomic population (the average number of electrons found in the atomic basin) is therefore simply the sum of diagonal elements of the AOM:

$$N(\mathrm{A}) = tr(\mathbf{S}^{\mathrm{A}}) \quad (8)$$

The off-diagonal elements of each AOM, however, provide valuable information regarding the 2nd-order density distribution across the atom, *i.e.* how MOs interfere (de)constructively within

Ω(A).[8,9] Such information can be used to indicate the degree of localization or delocalization of electrons within the atomic basin. Specifically, by integrating the pair density across two domains simultaneously, the total electron delocalization between electrons in each basin can be calculated:

$$\begin{aligned}\delta(\mathrm{A},\mathrm{B}) &= 2\left|-\sum_{ij}\int_{\mathrm{A}} d\mathbf{r}_1 \int_{\mathrm{B}} d\mathbf{r}_2\, \nu_i\nu_j\{\chi_i^*(\mathbf{r}_1)\chi_j\ (\mathbf{r}_1)\chi_j^*(\mathbf{r}_2)\chi_i\ (\mathbf{r}_2)\}\right| \\ &= 2\left|-\sum_{ij} S_{ij}^{\mathrm{A}} S_{ji}^{\mathrm{B}}\right|\end{aligned} \tag{9}$$

where we have used the definition for the elements of the AOM from Eq. 7. δ(A,B) is known as the delocalization index (DI)[10,11] for atom pair A,B. In single-determinant wavefunctions, it is often calculated by only considering spin-orbitals between parallel spin electrons, in order to calculate only the delocalization arising from Fermi correlation. Finally, note that the integrations can be swapped ($d\mathbf{r_1}$ over Ω(B), $d\mathbf{r_2}$ over Ω(A)) which will give the equivalent number of electrons, indicating that the number of electrons found on average in Ω(A) but delocalized into Ω(B) is the same as the number of electrons found on average in Ω(B) but delocalized into Ω(A); hence, the factor of 2 in Eq. 9.

Since Eq. 9 is written in terms of MOs, it is easy to recover the contribution of each MO and MO-pair to the total DI. A delocalized density matrix can be easily defined in terms of AOM elements:

$$D_{ij}^{(\mathrm{A},\mathrm{B})} = 2\left|-S_{ij}^{\mathrm{A}} S_{ji}^{\mathrm{B}}\right| \tag{10}$$

Diagonal elements of this matrix, $D_{ii}^{(\mathrm{A},\mathrm{B})}$, provides the contributions of each MO's contribution to the total number of electron pairs shared between A and B. However, the off-diagonal elements, $D_{i\neq j}^{(\mathrm{A},\mathrm{B})}$, provides the extent to which an MO-pair increases delocalized electron pairs (through constructive interference) or decreases delocalized electron pairs (through deconstructive interference). Therefore, the sum of any row or column of $\mathbf{D}_{ij}$ gives the net contribution of an MO to the number of electron pairs shared between atoms A and B, after any MO-pair interference effects have been taken into account.

MO	MO 1	MO 2	MO 3	MO 4	MO 5	MO 6	MO 7
MO 1	*1.00*	-1.00	0.00	0.00	0.00	0.00	0.00
MO 2	-1.00	*1.00*	0.00	0.00	0.00	0.00	0.00
MO 3	0.00	0.00	*1.00*	-0.27	0.00	0.00	0.00
MO 4	0.00	0.00	-0.27	*1.00*	-0.71	0.00	0.00
MO 5	0.00	0.00	0.00	-0.71	*1.00*	0.00	0.00
MO 6	0.00	0.00	0.00	0.00	0.00	*1.00*	0.00
MO 7	0.00	0.00	0.00	0.00	0.00	0.00	*1.00*
Sum	0.00	0.00	0.73	0.02	0.29	1.00	1.00
Percentage	0%	0%	24%	1%	10%	33%	33%

Figure S1.1. Delocalized matrix for N_2, as calculated at HF/6-311++G(2df,2pd) level.

For instance, consider the MOs in N_2, as calculated by HF/6-311++G(2df,2pd), shown in Figure S3.4. The delocalized matrix **D** is shown below, in Figure S1.1. The core $1s_N$ orbitals form a bonding and antibonding pair, χ_1 and χ_2. Both MOs contribute 1 electron pair to the total DI ($D_{11}^{(A,B)} = D_{22}^{(A,B)}$ = 1.0). However, the two orbitals are out-of-phase with each other, and interferes destructively so that $D_{12}^{(A,B)} = D_{21}^{(A,B)}$= –1.0. Therefore, the net contribution of MOs 1 and 2 is 0 electron pairs each. However, χ_3 – a σ-bonding MO – also contributes 1.0 electron pairs to the total DI, but interferes only weakly with χ_4 – a σ-antibonding MO. The net contribution of χ_3 is then 0.72 electron pairs. Finally, χ_4 interferes deconstructively with both χ_3 and χ_5 (the second σ-bonding MO), thereby bringing its net contribution down to only 0.02 electron pairs.

References

1. R. F. Bader. In *Atoms in molecules*; Wiley Online Library, **1990**.
2. S. Shahbazian. *Chem. Eur. J.* **2018**, *doi*: 10.1002/chem.201705163.
3. J. Contreras-García; E. R. Johnson; S. Keinan; R. Chaudret; J.-P. Piquemal; D. N. Beratan; W. Yang. *J. Chem. Theory Comput.* **2011**, *7*, 625-632.
4. A. Otero-de-la-Roza; E. R. Johnson; J. Contreras-García. *PCCP* **2012**, *14*, 12165-12172.
5. I. Cukrowski; J. H. de Lange; A. S. Adeyinka; P. Mangondo. *Comput. Theor. Chem.* **2015**, *1053*, 60-76.
6. J. H. de Lange; D. M. van Niekerk; I. Cukrowski. *J. Comput. Chem.* **2018**, *39*, 973-985.
7. J. H. Lange; I. Cukrowski. *J. Comput. Chem.* **2017**, *38*, 981-997.
8. R. F. Bader. *Monatshefte für Chemie/Chemical Monthly* **2005**, *136*, 819-854.
9. F. Cortés-Guzmán; R. F. Bader. *Coord. Chem. Rev.* **2005**, *249*, 633-662.
10. R. F. Bader; M. E. Stephens. *J. Am. Chem. Soc.* **1975**, *97*, 7391-7399.
11. R. Daudel; R. Bader; M. Stephens; D. Borrett. *Can. J. Chem.* **1974**, *52*, 1310-1320.

Part 2

XYZ coordinates of all optimized molecules

Table 2.1. Cartesian coordinates of H_2 (*eq*) dimer at rhf/6-311++g(2df,2pd) level.

Atom	X	Y	Z
H	0.000000	0.000000	0.367136
H	0.000000	0.000000	-0.367136

Table 2.2. Cartesian coordinates of H_2 (*eq*) dimer at rccsd(full)/6-311++g(2df,2pd) level.

Atom	X	Y	Z
H	0.000000	0.000000	0.371312
H	0.000000	0.000000	-0.371312

Table 2.3. Cartesian coordinates of CO (*eq*) dimer at rhf/6-311++g(2df,2pd) level.

Atom	X	Y	Z
C	0.000000	0.000000	-0.631980
O	0.000000	0.000000	0.471217

Table 2.4. Cartesian coordinates of CO (*eq*) dimer at rccsd(full)/6-311++g(2df,2pd) level.

Atom	X	Y	Z
C	0.000000	0.000000	-0.643051
O	0.000000	0.000000	0.482288

Table 2.5. Cartesian coordinates of N_2 (*eq*) dimer at rhf/6-311++g(2df,2pd) level.

Atom	X	Y	Z
N	0.000000	0.000000	0.533148
N	0.000000	0.000000	-0.533148

Table 2.6. Cartesian coordinates of N_2 (*eq*) dimer at rccsd(full)/6-311++g(2df,2pd) level.

Atom	X	Y	Z
N	0.000000	0.000000	0.547282
N	0.000000	0.000000	-0.547282

Table 2.7. Cartesian coordinates of Cr_2 (*eq*) dimer at b3lyp/6-311++g(2df,2pd) level.

Atom	X	Y	Z
Cr	0.000000	0.000000	0.878807
Cr	0.000000	0.000000	-0.878807

Table 2.8. Cartesian coordinates of Li_2H_2 (*eq*) at rhf/6-311++g(2df,2pd) level.

Atom	X	Y	Z
Li	0.000000	0.000000	-1.136802
H	0.000000	1.358612	0.000000
Li	0.000000	0.000000	1.136802
H	0.000000	-1.358612	0.000000

Table 2.9. Cartesian coordinates of Li_2H_2 (*eq*) at rccsd(full)/6-311++g(2df,2pd) level.

Atom	X	Y	Z
Li	0.000006	-1.127827	0.000000
H	-1.336426	-0.000012	0.000000
Li	0.000006	1.127831	0.000000
H	1.336391	0.000000	0.000000

Part 3

Data pertaining to the CO molecule

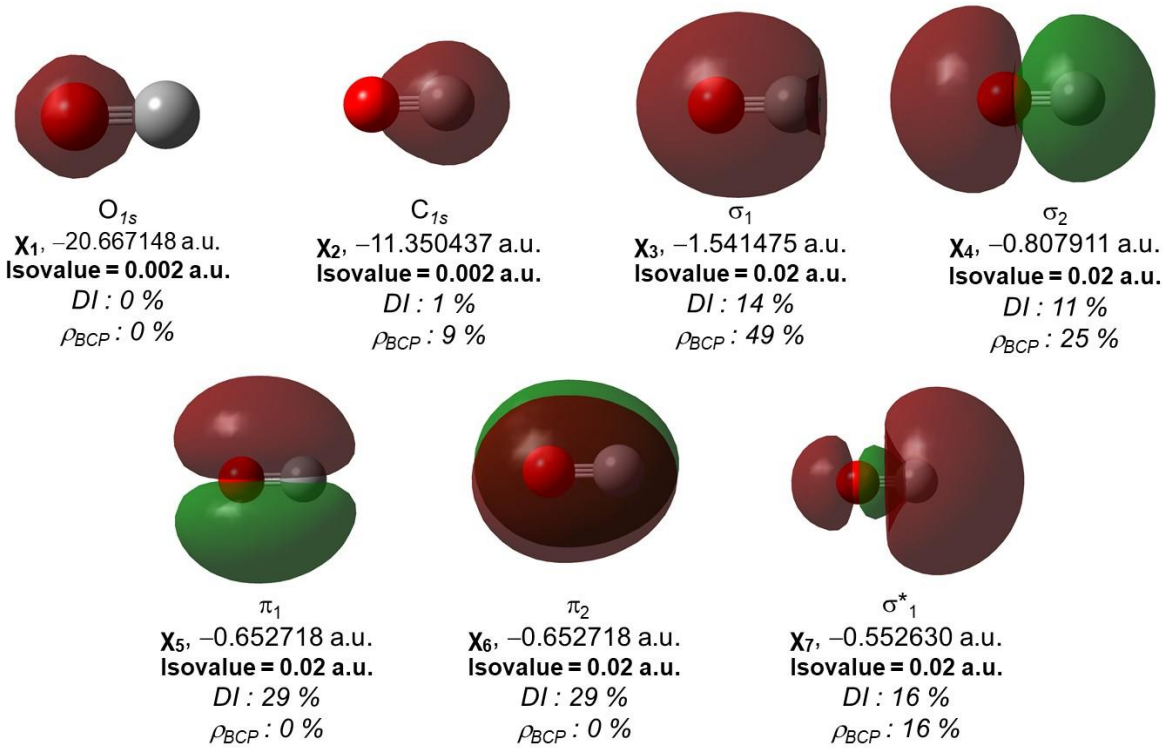

Figure 4.1. 3D-isosurfaces of MOs of CO at HF/6-311++G(2df,2pd) level. Percentage **c**ontributions to the *DI*(C,O) as well as to the electron density at the (3,–1) CP(C,O) are also shown.

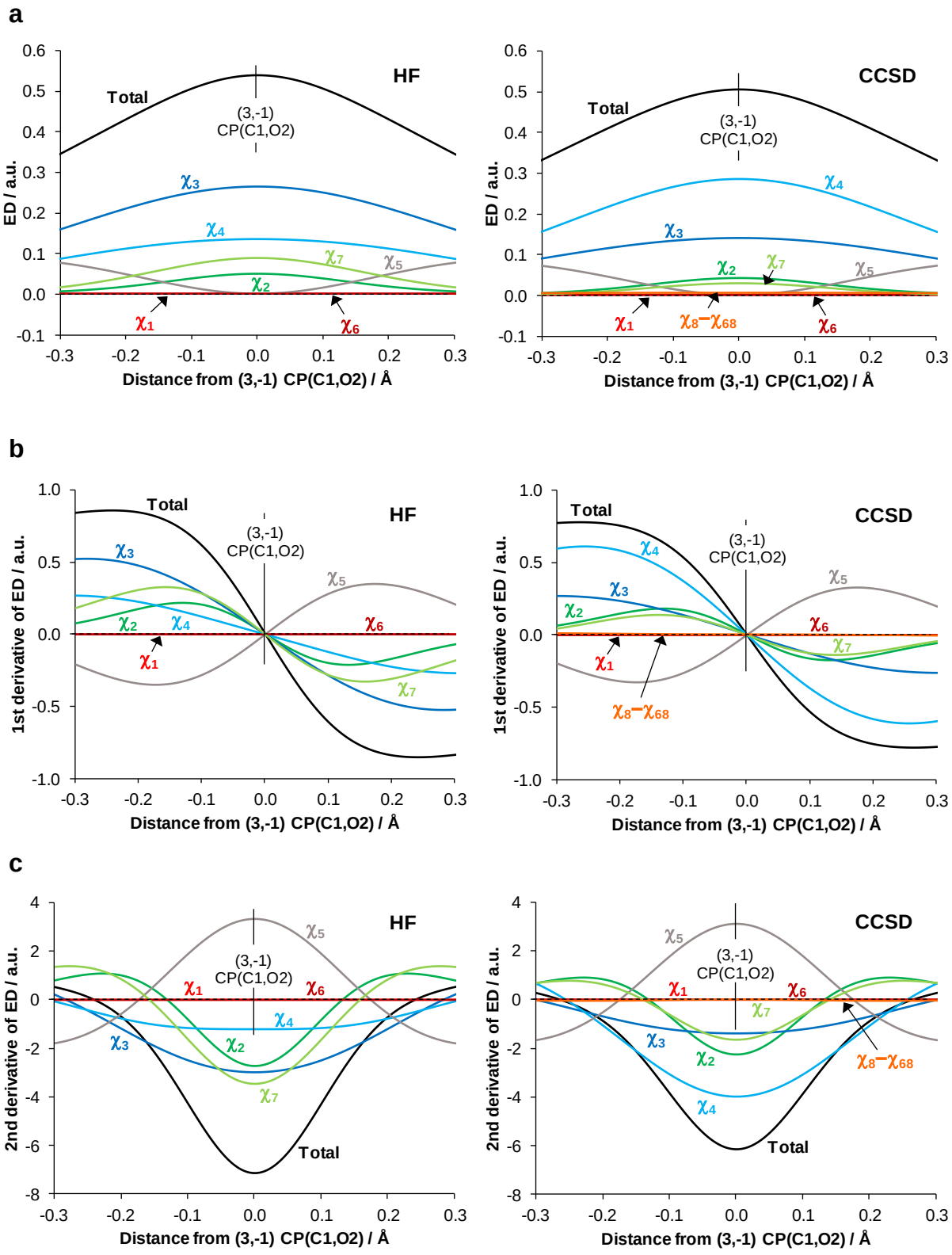

Figure 4.2. 1D-cross-sections along λ_2–eigenvector of MOs (HF) and NOs (CCSD) of CO. a) Total density contribution, b) directional partial 1st derivative and c) directional partial 2nd derivative.

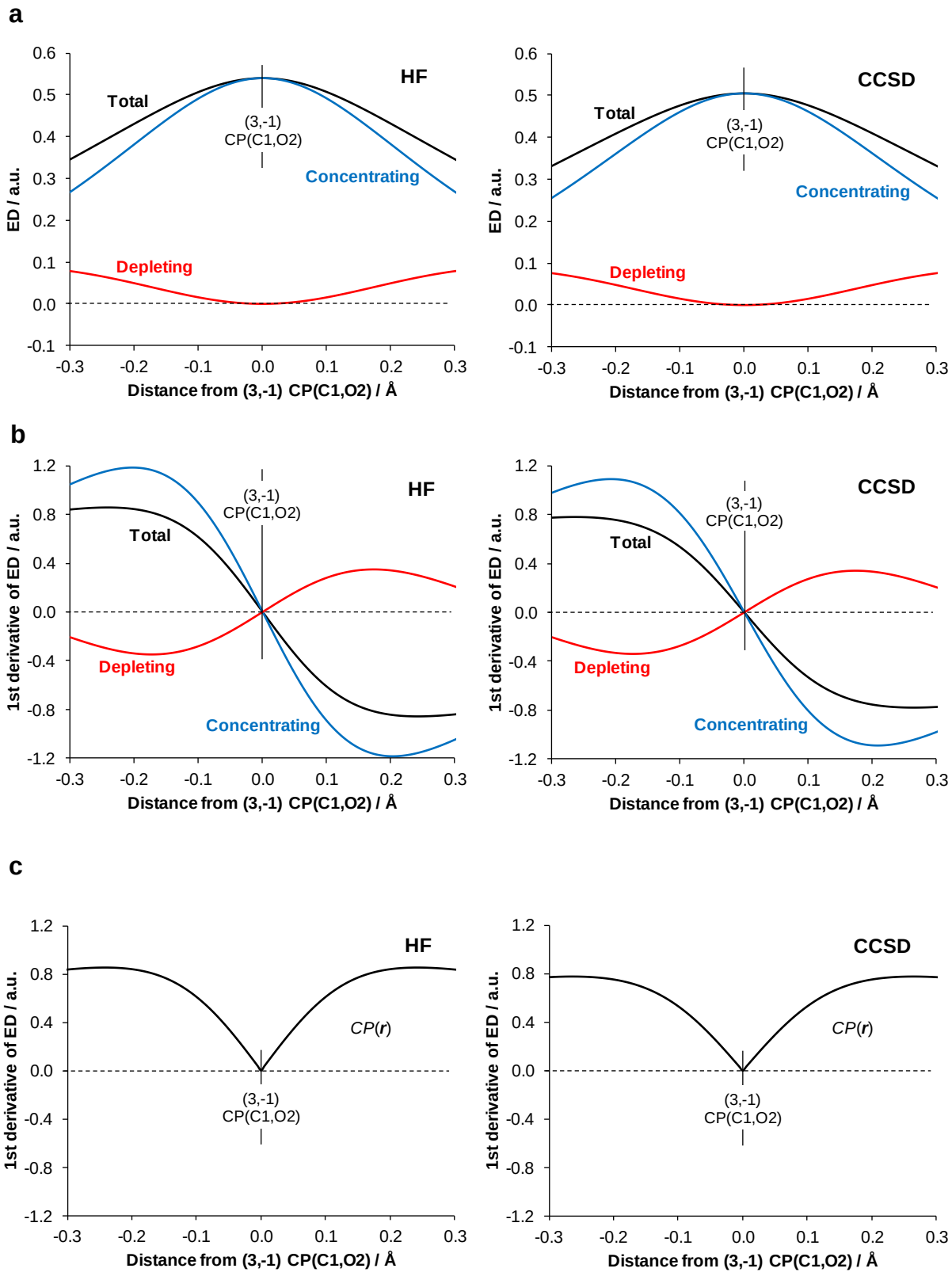

Figure 4.3. 1D-cross-sections along λ_2–eigenvector of MOs (HF) and NOs (CCSD) of CO with all concentrating or depleting orbitals grouped separately. a) Total density contribution, b) directional partial 1st derivative and c) *CP*(**r**) function.

Part 4

Data pertaining to the N_2 molecule

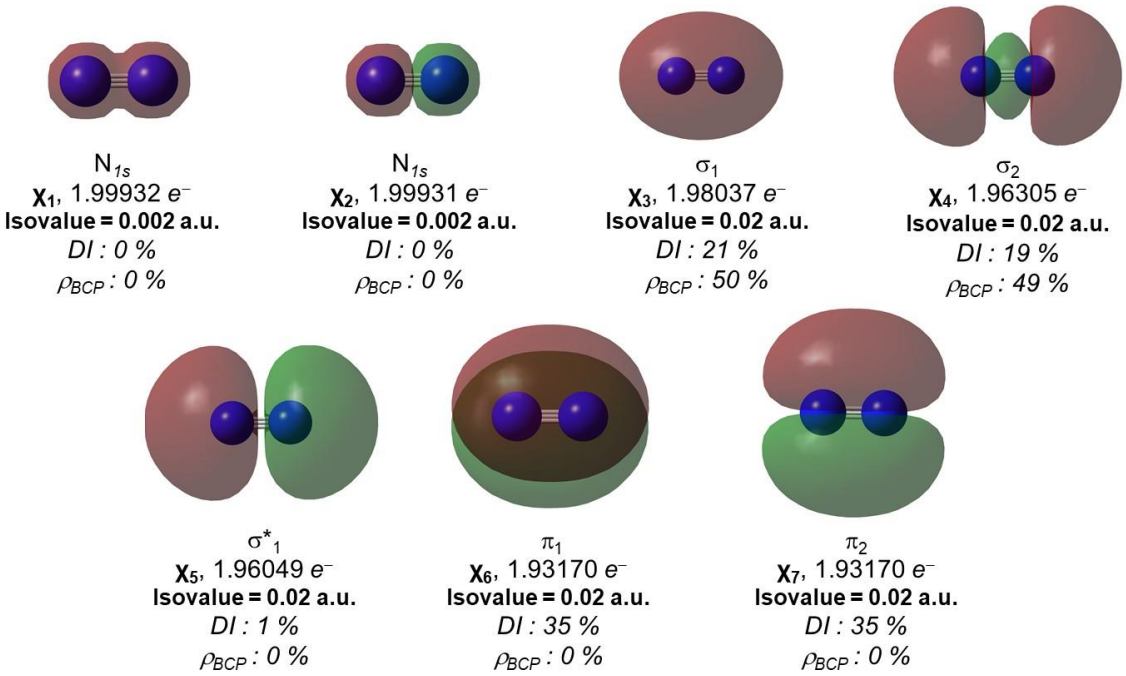

Figure 5.1. 3D-isosurfaces of selected NOs of N_2 at the CCSD/6-311++g(2df,2pd) level. Percentage **c**ontributions to the *DI*(N,N) as well as to the electron density at the (3,–1) CP(N,N) are also shown.

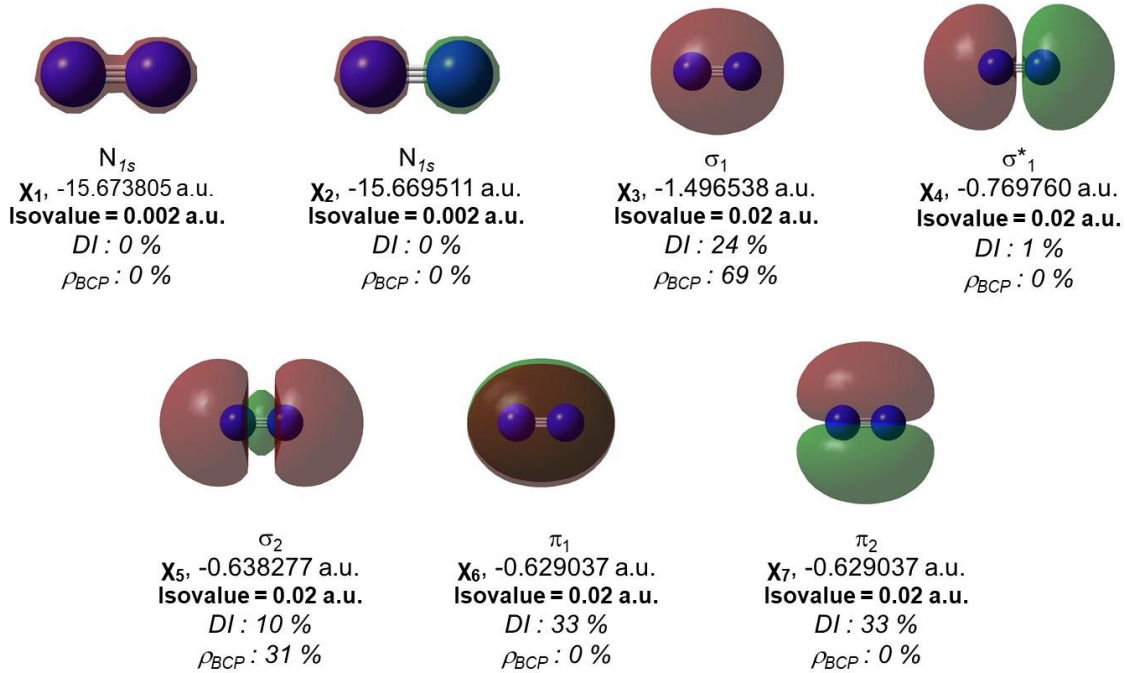

Figure 5.2. 3D-isosurfaces of MOs of N_2 at the HF/6-311++g(2df,2pd) level. Percentage **c**ontributions to the *DI*(N,N) as well as to the electron density at the (3,–1) CP(N,N) are also shown.

Table 5.1. Molecular orbital contributions and their classifications in terms of bonding in N_2 at the CCSD (Part a) and HF (Part b) levels.

Part a. Data at the CCSD level

Orbital	Electron population (N) / e^-		Orthodox		At (3,-1) Critical point {N1,N2}			Delocalisation index		
			Label	Classification based on AO interference	ED contribution / ρ		Classification based on 2nd derivative sign (λ_2)	Contribution / e^- pairs		Classification based on MO interference[a]
$\chi1$	1.99932	(14.3%)	N_{1s}	nonbonding	0.00063	(0.1%)	concentrating	0.00003	(0.0%)	constructive
$\chi2$	1.99931	(14.3%)	N_{1s}	nonbonding	0.00000	(0.0%)	non-contributing	0.00003	(0.0%)	constructive
$\chi3$	1.98037	(14.1%)	σ_1	bonding	0.35660	(50.3%)	concentrating	0.48802	(21.0%)	constructive
$\chi4$	1.96305	(14.0%)	σ_2	bonding	0.34861	(49.2%)	concentrating	0.44842	(19.3%)	constructive
$\chi5$	1.96049	(14.0%)	σ^*_1	antibonding	0.00000	(0.0%)	non-contributing	0.01853	(0.8%)	constructive
$\chi6$	1.93170	(13.8%)	π_1	bonding	0.00000	(0.0%)	depleting[b]	0.82419	(35.5%)	constructive
$\chi7$	1.93170	(13.8%)	π_2	bonding	0.00000	(0.0%)	depleting	0.82419	(35.5%)	constructive
$\chi8$–$\chi68$	0.23406	(1.7%)	–	–	0.00334	(0.5%)	–	-0.28128	(-12.1%)	destructive
Total	14.00000	(100.0%)	–	bond order = 3	0.70917	(100.0%)	DB {N1,N2} present	2.32213	(100.0%)	–

Part b. Data at the HF level.

Orbital	Hartree Fock energy / a.u.	Orthodox		At (3,-1) Critical point {N1,N2}			Delocalisation index		
		Label	Classification based on AO interference	ED contribution / ρ		Classification based on 2nd derivative sign (λ_2)	Contribution / e^- pairs		Classification based on MO interference[a]
$\chi1$	-15.673805	N_{1s}	nonbonding	0.00120	(0.2%)	concentrating	0.00008	(0.0%)	constructive
$\chi2$	-15.669511	N_{1s}	nonbonding	0.00000	(0.0%)	non-contributing	0.00004	(0.0%)	constructive
$\chi3$	-1.496538	σ_1	bonding	0.53511	(69.1%)	concentrating	0.72884	(24.0%)	constructive
$\chi4$	-0.769760	σ^*_1	antibonding	0.00000	(0.0%)	non-contributing	0.02134	(0.7%)	constructive
$\chi5$	-0.638277	σ_2	bonding	0.23812	(30.7%)	concentrating	0.29245	(9.6%)	constructive
$\chi6$	-0.629037	π_1	bonding	0.00000	(0.0%)	depleting[b]	1.00000	(32.9%)	constructive
$\chi7$	-0.629037	π_2	bonding	0.00000	(0.0%)	depleting	1.00000	(32.9%)	constructive
Total	–	–	bond order = 3	0.77443	(100.0%)	DB {N1,N2} present	2.32213	(100.0%)	–

[a] positive value = constructive interference, negative value = destructive interference

[b] non-contributing orbital $\chi6$ is degenerate with orbital $\chi7$, depleting along λ_1

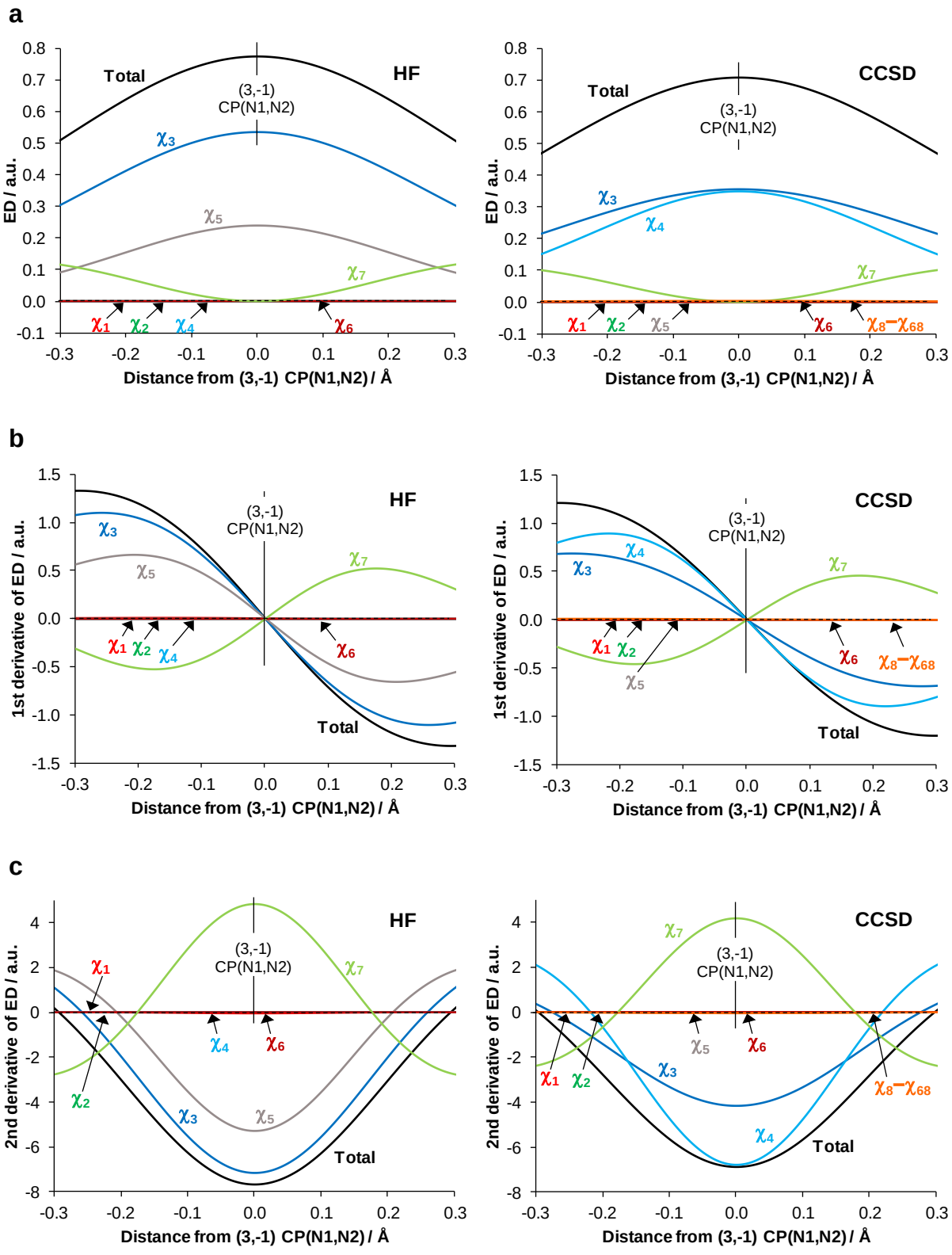

Figure 5.3. 1D-cross-sections along λ_2–eigenvector of MOs (HF) and NOs (CCSD) of N_2. a) Total density contribution, b) directional partial 1st derivative and c) directional partial 2nd derivative.

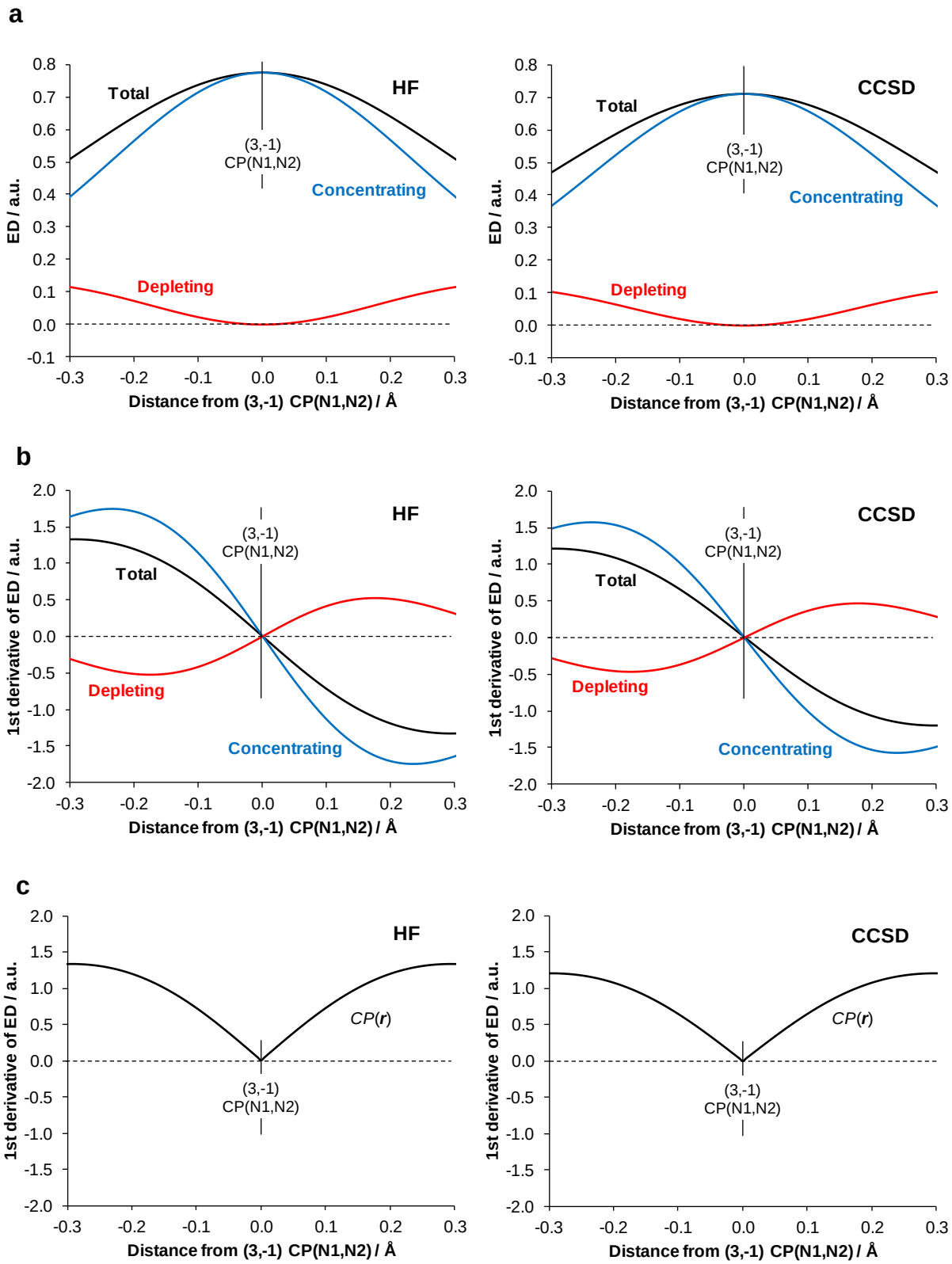

Figure 5.4. 1D-cross-sections along λ_2–eigenvector of MOs (HF) and NOs (CCSD) of N_2 with all concentrating or depleting orbitals grouped separately**.** a) Total density contribution, b) directional partial 1st derivative and c) *CP*(**r**) function.

Part 5

Data pertaining to the H_2 molecule

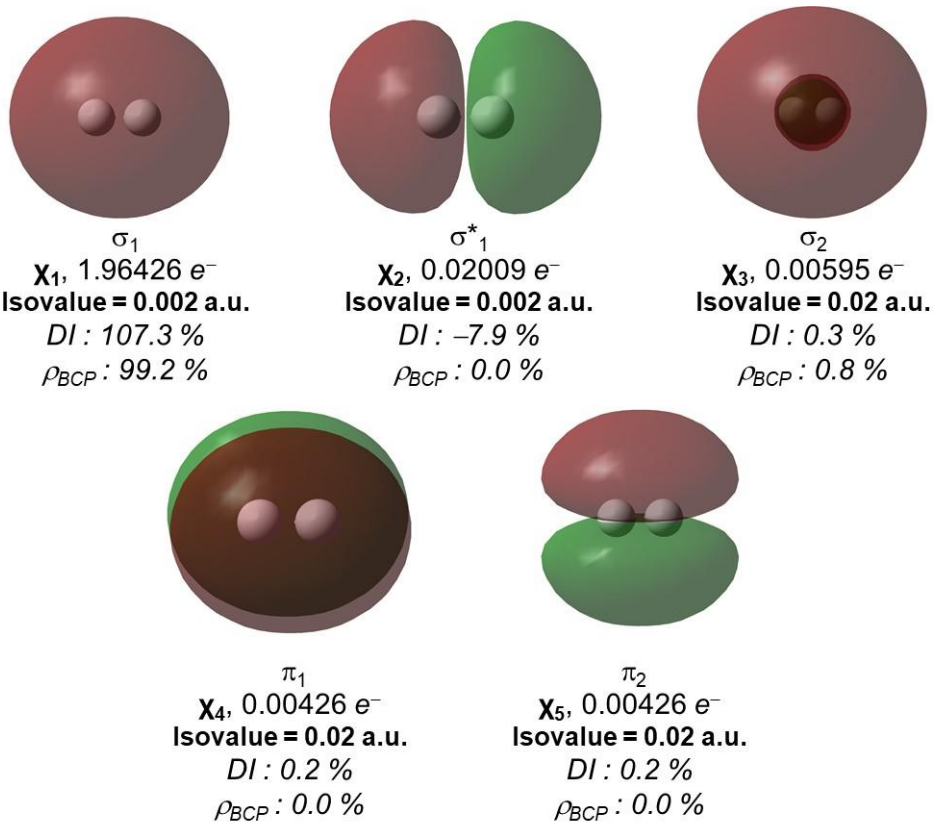

Figure 6.1. 3D-isosurfaces of selected NOs in H_2 at the CCSD/6-311++G(2df,2pd) level. Percentage **c**ontributions to the *DI*(H,H) as well as to the electron density at the (3,–1) CP(H,H) are also shown.

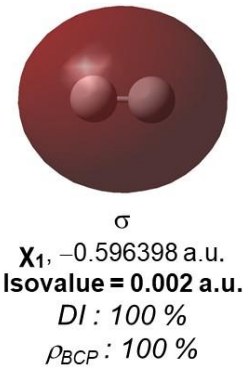

Figure 6.2. 3D-isosurface of the occupied MO in H_2 at the HF/6-311++G(2df,2pd) level. Percentage **c**ontributions to the *DI*(H,H) as well as to the electron density at the (3,–1) CP(H,H) are also shown.

Table 6.1. Molecular orbital contributions and their classifications in terms of bonding in CO at the CCSD and HF levels.

Orbital	Electron population (N) / e^-	Hartree Fock energy / a.u.	Orthodox		At (3,-1) Critical point {H1,H2}		Delocalisation index	
			Label	Classification based on AO interference	ED contribution / ρ	Classification based on 2nd derivative sign (λ_2)	Contribution / e^- pairs	Classification based on MO interference[a]
$\chi 1$	1.96426 (98.2%)	-0.60	H_{1s}	bonding	0.26636 (99.2%)	concentrating	0.90555 (107.3%)	constructive
$\chi 2$–$\chi 30$	0.03574 (1.8%)	–	–	–	0.00211 (0.8%)	–	-0.06125 (-7.3%)	destructive
Total	2.00000 (100.0%)	–	–	bond order = 1	0.26847 (100.0%)	DB {H1,H2} present	0.84430 (100.0%)	–

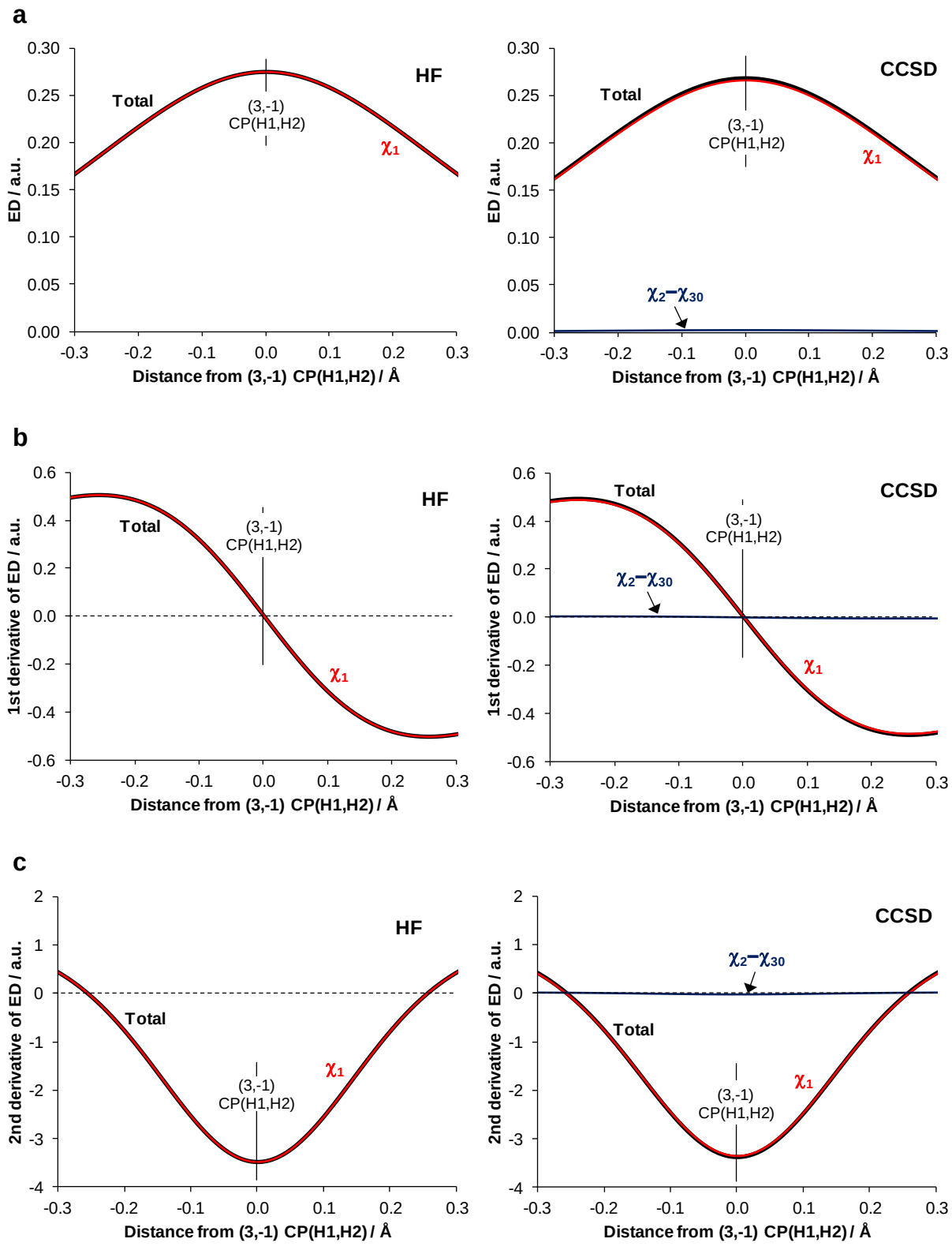

Figure 6.3. 1D-cross-sections along λ_2–eigenvector of MOs (HF) and NOs (CCSD) of H_2. a) Total density contribution, b) directional partial 1st derivative and c) directional partial 2nd derivative.

Part 6

Data pertaining to the Cr_2 molecule

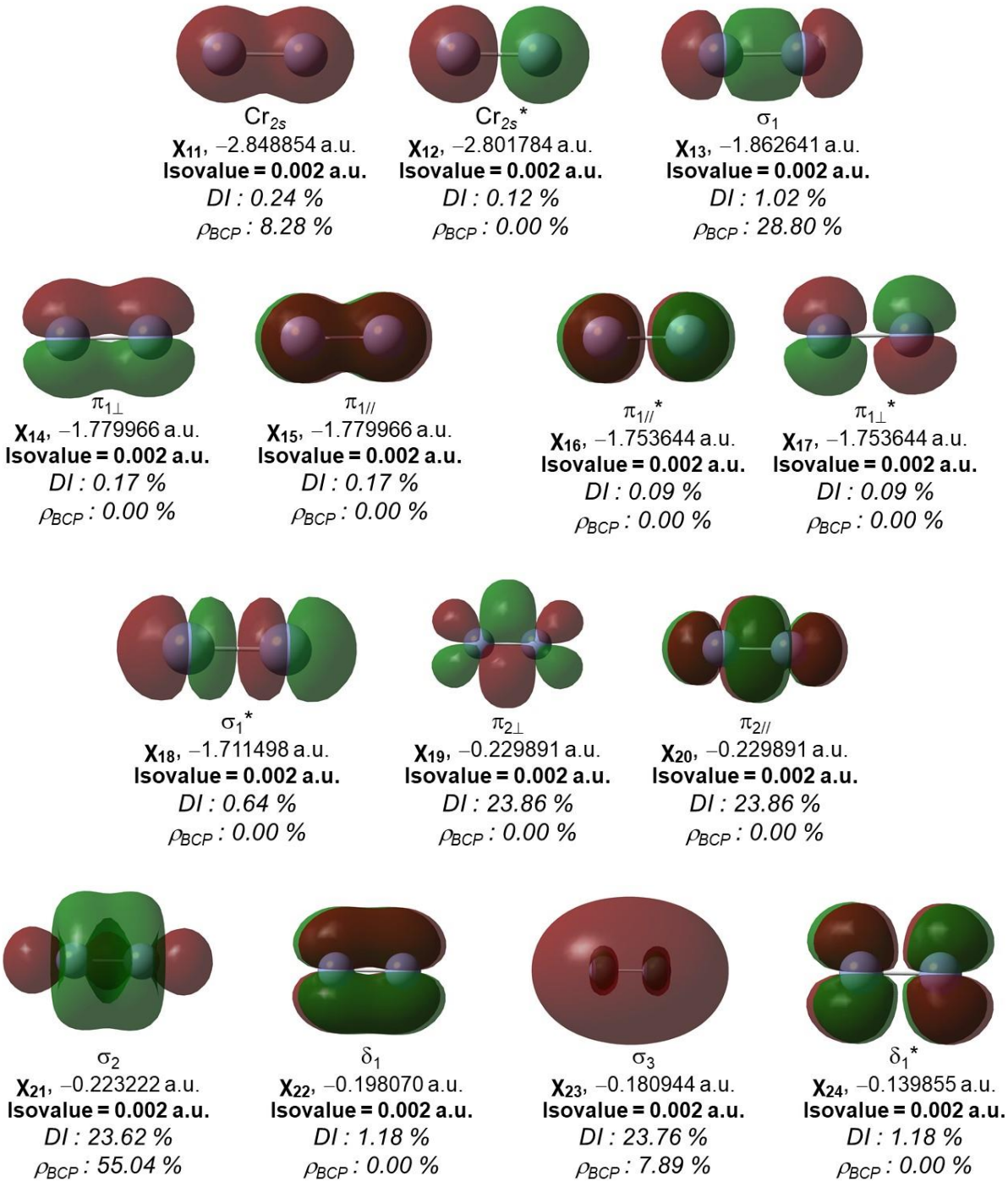

Figure 7.1. 3D-isosurfaces of selected MOs in Cr_2 at the B3LYP/6-311++G(2df,2pd) level. Percentage **c**ontributions to the *DI*(Cr,Cr) as well as to the electron density at the (3,–1) CP(Cr,Cr) are also shown.

Table 7.1. Molecular orbital contributions and their classifications in terms of bonding in in Cr_2 at the B3LYP/6-311++G(2df,2pd) level.

Orbital	B3LYP energy / a.u.	Orthodox		At (3,-1) Critical point {Cr1,Cr2}			Delocalisation index		
		Label	Classification based on AO interference	ED contribution / ρ		Classification based on 2nd derivative sign (λ_2)	Contribution / e^- pairs		Classification based on MO interference[a]
$\chi 1 - \chi 10$		Core	nonbonding	0.00000	(0.0%)	non-contributing	0.00000	(0.0%)	non-contributing
$\chi 11$	-2.848855	Cr_{2s}	bonding	0.02052	(8.3%)	concentrating	0.01017	(0.2%)	constructive
$\chi 12$	-2.801784	Cr_{2s}^*	antibonding	0.00000	(0.0%)	non-contributing	0.00495	(0.1%)	constructive
$\chi 13$	-1.862641	σ_1	bonding	0.07138	(28.8%)	concentrating	0.04256	(1.0%)	constructive
$\chi 14$	-1.779966	$\pi_{1\perp}$	bonding	0.00000	(0.0%)	depleting	0.00719	(0.2%)	constructive
$\chi 15$	-1.779966	$\pi_{1//}$	bonding	0.00000	(0.0%)	non-contributing	0.00719	(0.2%)	constructive
$\chi 16$	-1.753644	$\pi_{1//}^*$	antibonding	0.00000	(0.0%)	non-contributing	0.00370	(0.1%)	constructive
$\chi 17$	-1.753644	$\pi_{1\perp}^*$	antibonding	0.00000	(0.0%)	non-contributing	0.00370	(0.1%)	constructive
$\chi 18$	-1.711498	σ^*_1	antibonding	0.00000	(0.0%)	non-contributing	0.02680	(0.6%)	constructive
$\chi 19$	-0.229891	$\pi_{2\perp}$	bonding	0.00000	(0.0%)	depleting	0.99650	(23.9%)	constructive
$\chi 20$	-0.229891	$\pi_{2//}$	bonding	0.00000	(0.0%)	non-contributing	0.99650	(23.9%)	constructive
$\chi 21$	-0.223222	σ_2	bonding	0.13643	(55.0%)	concentrating	0.98669	(23.6%)	constructive
$\chi 22$	-0.198070	δ_1	bonding	0.00000	(0.0%)	non-contributing	0.04913	(1.2%)	constructive
$\chi 23$	-0.180944	σ_3	bonding	0.01955	(7.9%)	concentrating	0.99231	(23.8%)	constructive
$\chi 24$	-0.139855	δ_1^*	antibonding	0.00000	(0.0%)	non-contributing	0.04913	(1.2%)	constructive
Total	–	–	bond order ~ 4	0.24787	(100.0%)	DB {Cr1,Cr2} present	4.17653	(100.0%)	–

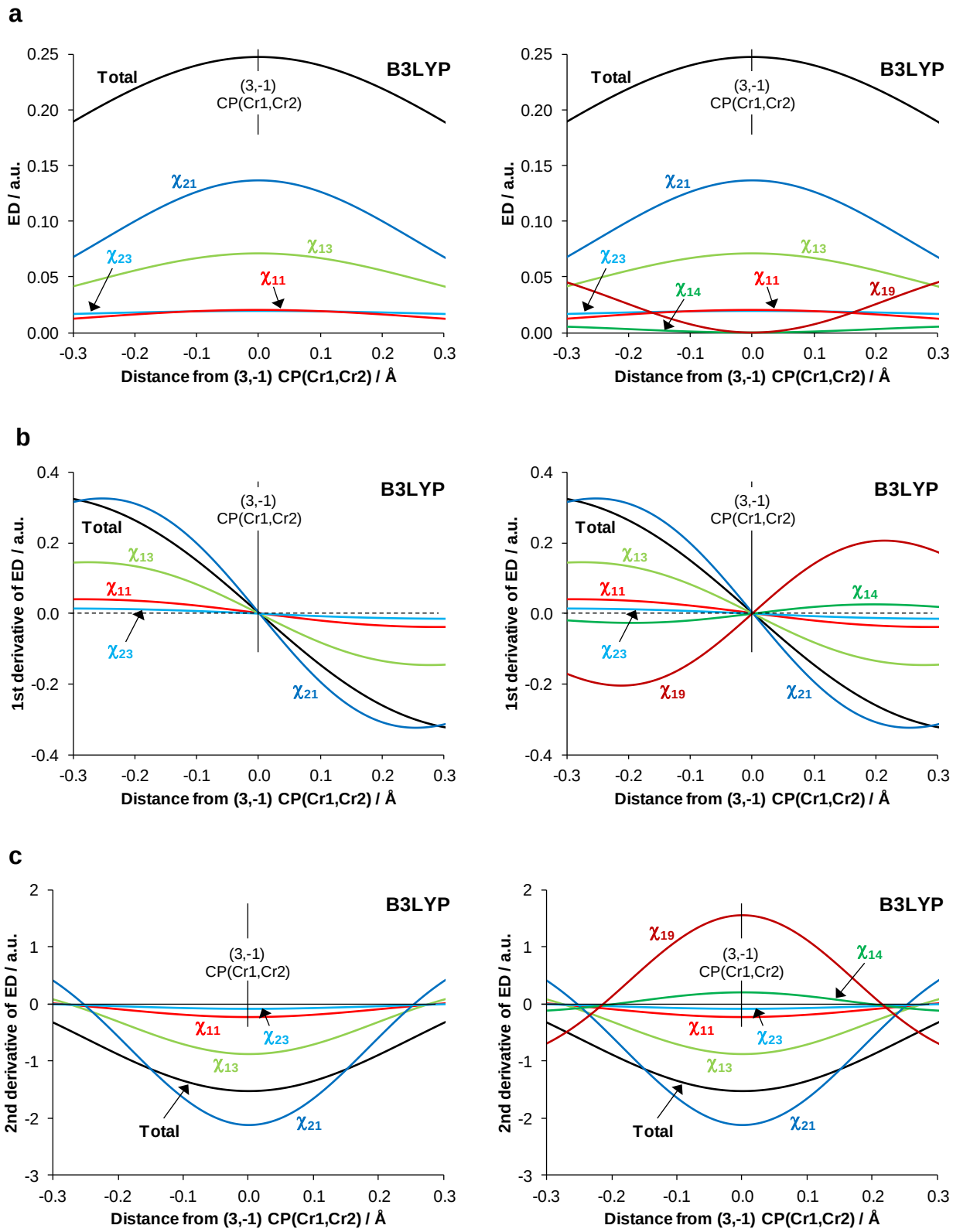

Figure 7.2. 1D-cross-sections along λ_2–eigenvector of σ-bonding MOs as well as highest-contributing MOs of Cr_2 at the B3LYP/6-311++G(2df,2pd) level. a) Total density contribution, b) directional partial 1st derivative and c) directional partial 2nd derivative.

Part 7

Data pertaining to the LiH dimer

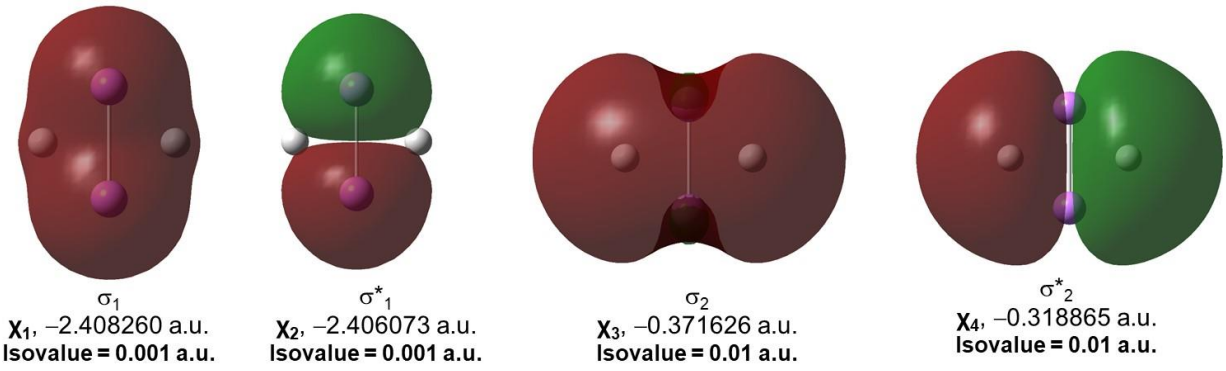

Figure 7.1. 3D-isosurfaces of MOs of Li_2H_2 at the HF/6-311++G(2df,2pd) level.

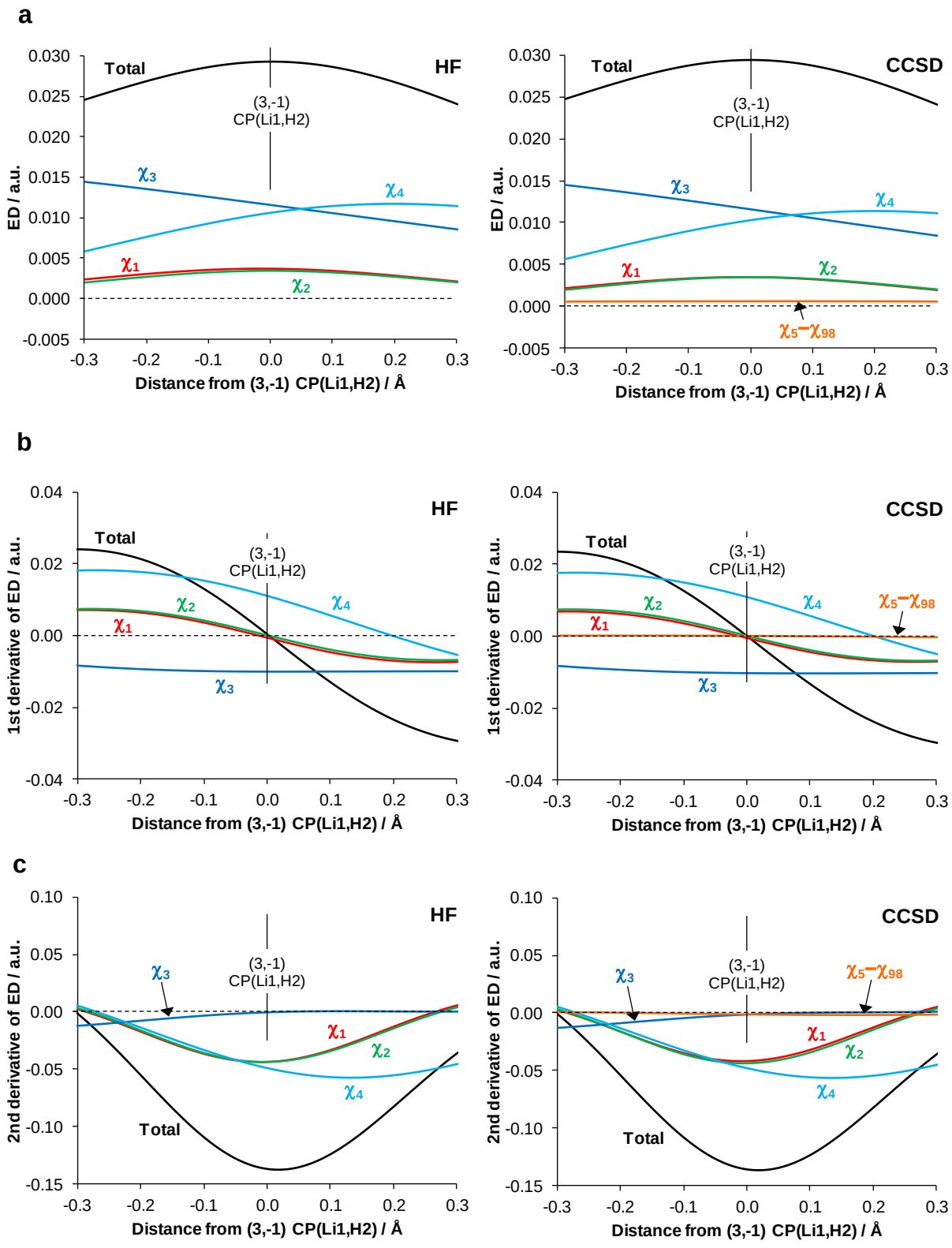

Figure 7.2. 1D-cross-sections along $\nu_{Li1\perp H2}$ of MOs (HF) and NOs (CCSD) of the Li_2H_2 molecule. a) Total density contribution, b) directional partial 1st derivative and c) directional partial 2nd derivative.

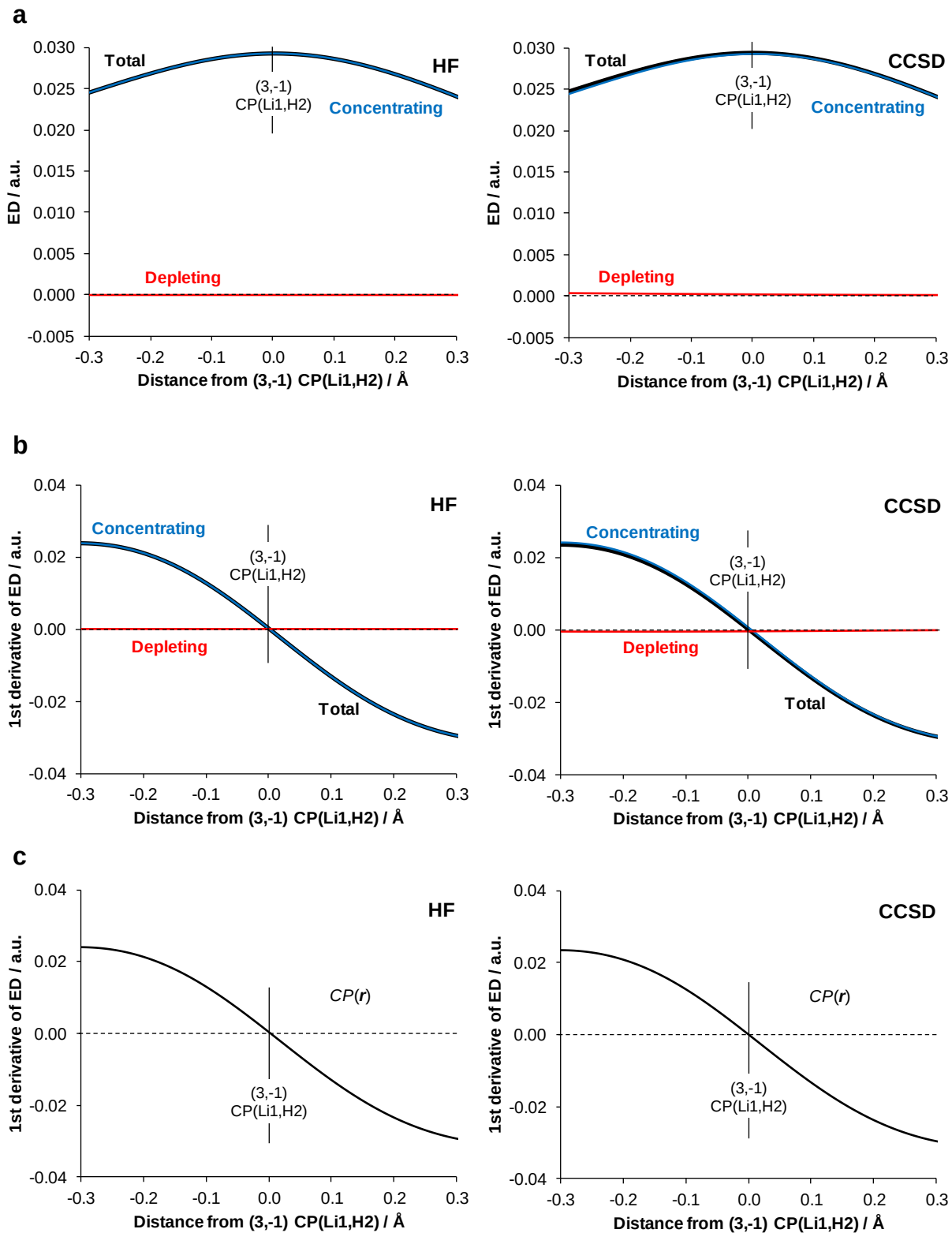

Figure 7.3. 1D-cross-sections along $\nu_{Li1\perp H2}$ of MOs (HF) and NOs (CCSD) of the Li_2H_2 molecule with all concentrating or depleting orbitals grouped separately. a) Total density contribution, b) directional partial 1st derivative and c) *CP*(**r**) function.

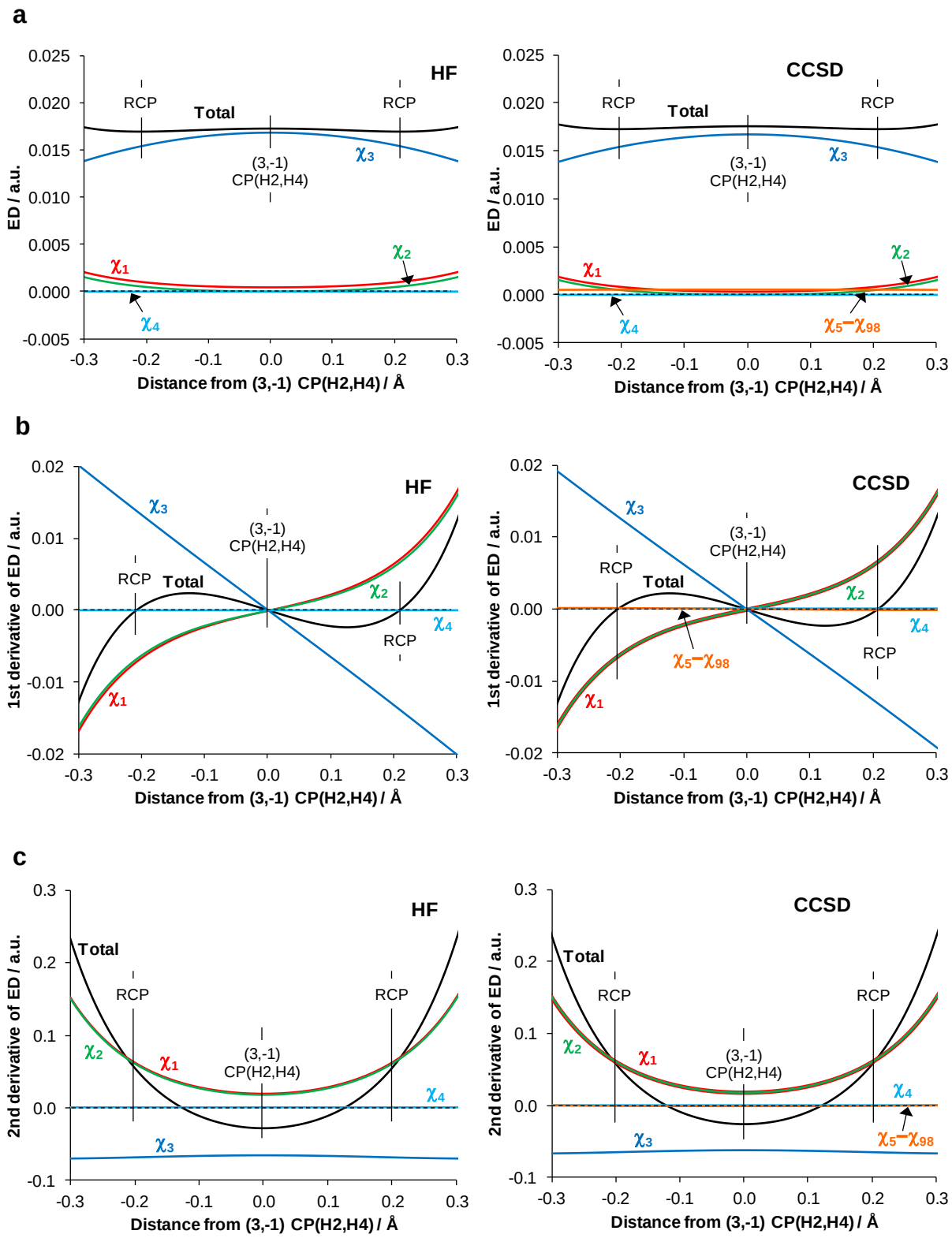

Figure 7.4. 1D-cross-sections along $\nu_{H2\perp H4}$ of MOs (HF) and NOs (CCSD) of the Li_2H_2 molecule. a) Total density contribution, b) directional partial 1st derivative and c) directional partial 2nd derivative.

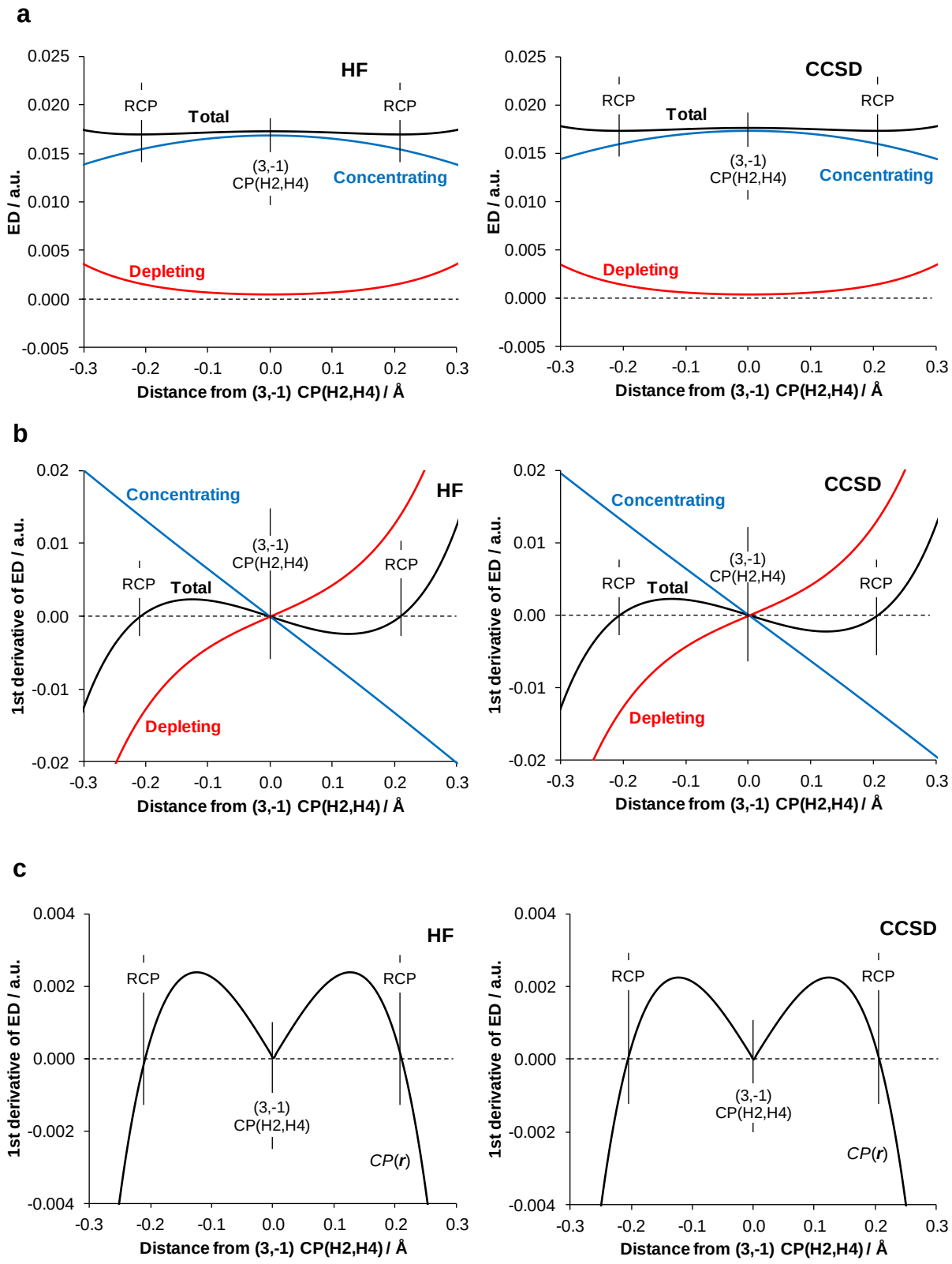

Figure 7.5. 1D-cross-sections along $\nu_{H2\perp H4}$ of MOs (HF) and NOs (CCSD) of the Li_2H_2 molecule with all concentrating or depleting orbitals grouped separately. a) Total density contribution, b) directional partial 1st derivative and c) *CP*(**r**) function.

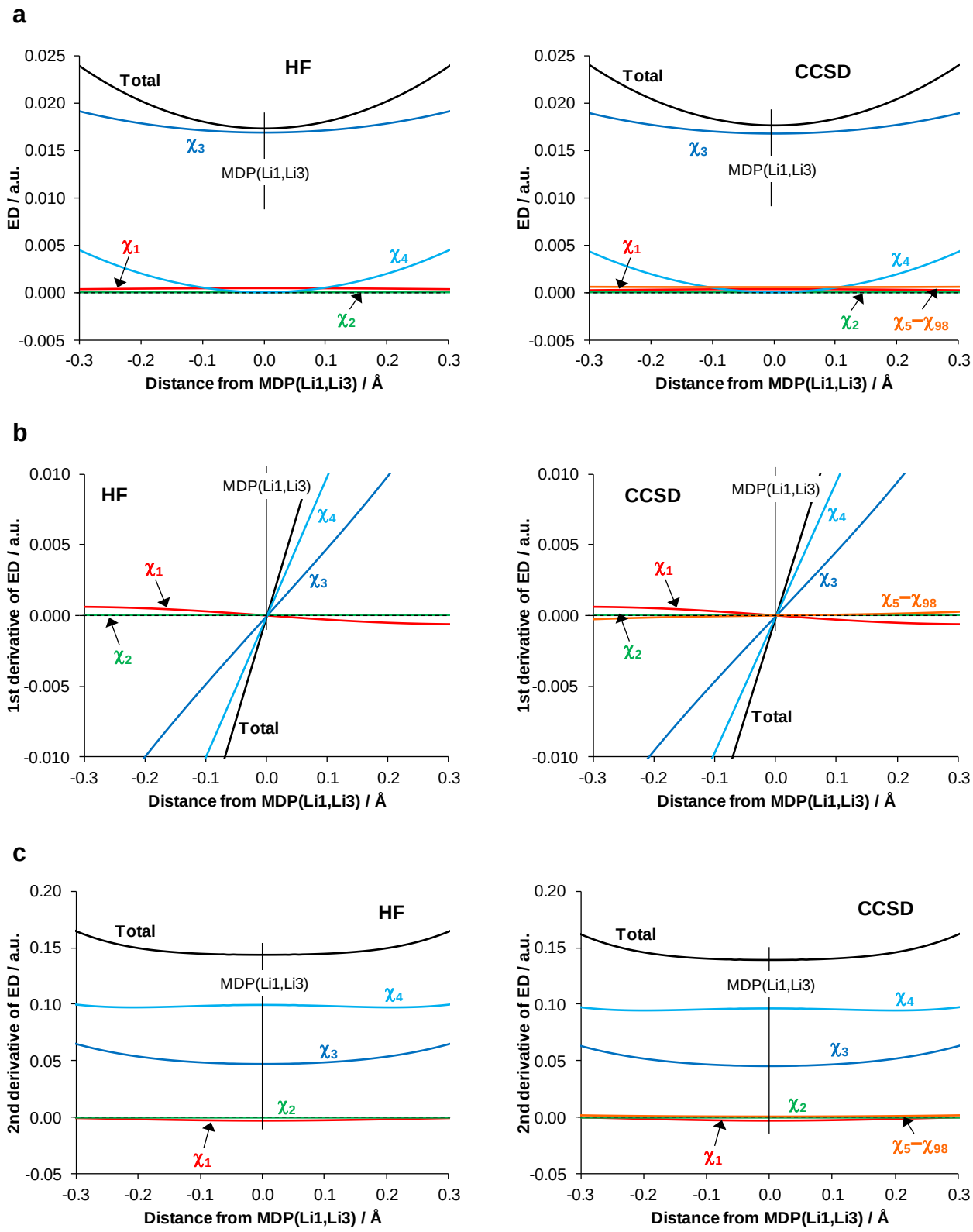

Figure 7.6. 1D-cross-sections along $\nu_{Li1\perp Li3}$ of MOs (HF) and NOs (CCSD) of the Li_2H_2 molecule. a) Total density contribution, b) directional partial 1st derivative and c) directional partial 2nd derivative.

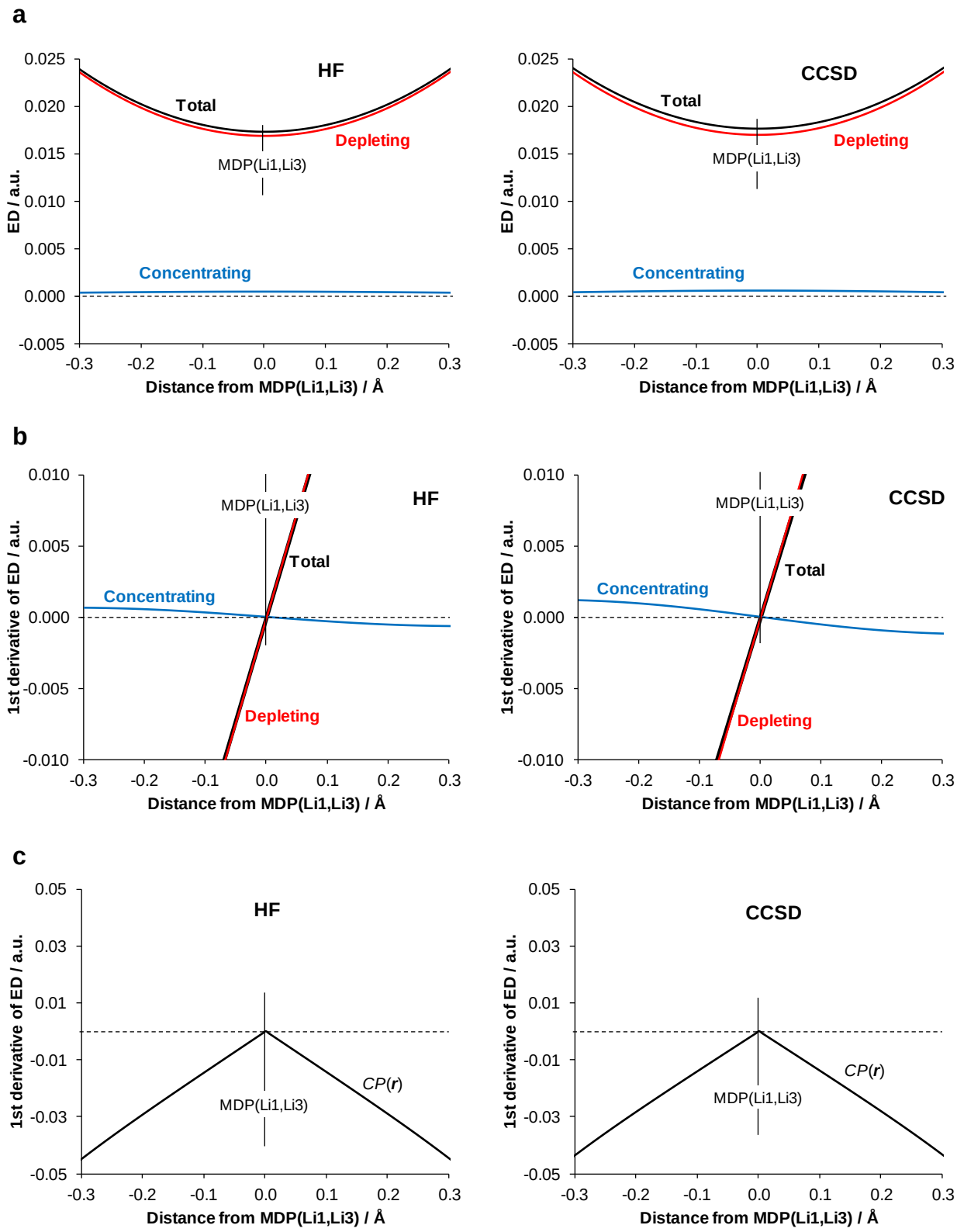

Figure 7.7. 1D-cross-sections along $\nu_{Li1\perp Li3}$ of MOs (HF) and NOs (CCSD) of the Li_2H_2 molecule with all concentrating or depleting orbitals grouped separately. a) Total density contribution, b) directional partial 1st derivative and c) *CP*(**r**) function.